A new reconstruction of multituberculate endocranial casts and encephalization quotient of *Kryptobaatar*

ZOFIA KIELAN-JAWOROWSKA and TERRY E. LANCASTER

Z. Kielan-Jaworowska and T.E. Lancaster. 2004. A new reconstruction of multituberculate endocranial casts and encephalization quotient of *Kryptobaatar*. *Acta Palaeontologica Polonica* 49 (2) 177–188.

Multituberculate and eutriconodontan endocasts differ from those of primitive therian mammals in their lack of visible midbrain exposure on the dorsal side and in having a vermis-like triangular bulge (recognized herein as the cast of a large sinus—the superior cistern) inserted between the cerebral hemispheres. As the shape and proportions of multituberculate, eutriconodontan, and Cretaceous eutherian endocasts are otherwise similar, one might speculate that the multituberculate and eutriconodontan brains did not differ essentially from those of primitive eutherian and marsupial mammals, in which the midbrain is exposed dorsally. This conclusion might have important phylogenetic implications, as multituberculates and eutriconodontans may lay closer to the therians *sensu strico*, than hitherto believed. We describe an endocast of the Late Cretaceous multituberculate *Kryptobaatar*, which differs from those of other multituberculates (*Ptilodus*, *Chulsanbaatar*, and *Nemegtbaatar*) in having unusually long olfactory bulbs and the paraflocculi elongated transversely, rather than ball-shaped. We estimate the encephalization quotient (EQ) of *Kryptobaatar*, using: 1) Jerison's classical equation (1) based on estimation of endocranial volume and body mass; 2) McDermott et al.'s derived body mass estimation equation (2) using upper molar lengths; and 3) estimation of body mass based on new equations (3a, 3b, 3c, and $3d_{1–9}$), which we propose, using measurements of the humerus, radius, ulna, femur and tibia. In both Jerison's method and a mean of our series of derived formulae, the EQ varies around 0.71, which is higher than estimated for other multituberculate mammals. It remains an open question whether the evolutionary success of *Kryptobaatar* (which was a dominant mammal during the ?early Campanian on the Gobi Desert and survived until the ?late Campanian) might have been related to its relatively high EQ and well developed sensorimotor adaptations, in particular olfaction and coordinated movements.

Key words: Multituberculata, *Kryptobaatar*, brain structure, endocasts, superior cistern, encephalization quotient, body mass, Late Cretaceous, Mongolia.

Zofia Kielan-Jaworowska [zkielan@twarda.pan.pl], Instytut Paleobiologii PAN, ul. Twarda 51/55, PL-00-818 Warszawa, Poland;
Terry E. Lancaster [tlancast@neoucom.edu], Northeastern Ohio Universities College of Medicine, 4209 State Route 44, PO Box 95, Rootstown, Ohio 44272-0095, USA.

Introduction

In 1937, George Gaylord Simpson reconstructed the first multituberculate brain on the basis of several endocranial casts (endocasts) of Paleocene *Ptilodus*. More than thirty years later, Hahn (1969) reconstructed the dorsal aspect of the endocast of the Late Jurassic *Paulchoffatia* on the basis of the skull structure and a comparison with the reconstructed endocast of *Ptilodus*. The endocast of *Paulchoffatia*, however, has remained unknown. In Simpson's (1937) reconstruction of the *Ptilodus* endocast, the olfactory bulbs widen anteriorly, which is unusual for mammals. Krause and Kielan-Jaworowska (1993) revised the material described by Simpson and demonstrated that the olfactory bulbs in *Ptilodus* tapered anteriorly, as in all other mammals.

New data on multituberculate endocasts, with appropriate inferences about the brain, came from study of Late Cretaceous specimens from Mongolia. Kielan-Jaworowska (1974) figured dorsal aspects of several natural endocasts preserved in *Chulsanbaatar* from the Baruungoyot Formation (?upper Campanian), one of which was mistakenly identified as ?*Kamptobaatar*. Subsequently (1983), by removal of all the bones and cutting off the cast of the nasal cavity, she developed from the skull of *Chulsanbaatar* the complete, three-dimensional endocast. Further information was obtained from the study of the serially sectioned skulls of *Nemegtbaatar* and *Chulsanbaatar* by Kielan-Jaworowska et al. (1986). These authors reconstructed the brain of *Nemegtbaatar*, based on a wax model constructed on the basis of serial sections, and provided an emended reconstruction of the endocast in *Chulsanbaatar*, on the basis of comparisons with *Nemegtbaatar*. Kielan-Jaworowska (1986) argued that in brains of Cretaceous multituberculates and therians the neocortex was apparently developed.

In this paper, at the suggestion of Harry J. Jerison, we offer a new interpretation of multituberculate endocasts, interpreting the structure previously referred to as the vermis, as a cast of a large sinus, which on the endocasts obscured the vermis and probably also the midbrain. We also describe an endocast of the Late Cretaceous multituberculate mammal

Kryptobaatar and make an attempt at evaluating its encephalization quotient (EQ), using three different methods of calculating its body mass.

Institutional abbreviations.—AMNH, American Museum of Natural History, New York; CM, Carnegie Museum of Natural History, Pittsburgh; GI PST, Paleontological and Stratigraphic Section of the Geological Institute, Mongolian Academy of Sciences, Ulaanbaatar; IMM, Inner Mongolian Museum, Hohhot, China; NMNH, National Museum of Natural History, Smithsonian Institution, Washington, D.C.; PM, Paleontological Center of the Mongolian Academy of Sciences, Ulaanbaatar; PSS-MAE, collection assembled by the Mongolian-American Museum Expeditions, housed at the American Museum of Natural History in New York; THEW, J.G.M. Thewissen's personal skeletal collection, Rootstown, Ohio. UMMZ, University of Michigan Museum of Zoology, Ann Arbor, Michigan; USNM, United States National Museum, Washington, D.C.; ZPAL, Institute of Paleobiology of the Polish Academy of Sciences, Warsaw.

Vermis *versus* superior cistern

Simpson (1937), who was the first to reconstruct the multituberculate endocast (of *Ptilodus*), referred to the triangular bulge, inserted between the cerebral hemispheres as the "central lobe of the cerebellum" (= vermis). He was followed in this respect by the students of multituberculate endocasts (e.g., Jerison 1973; Hahn 1969; Kielan-Jaworowska 1983, 1986, 1997; Kielan-Jaworowska et al. 1986; Krause and Kielan-Jaworowska 1993).

Bauchot and Stephan (1967) demonstrated how the endocranial casts of extant insectivores *sensu lato* differ from their actual brains. Using the modern brain terminology for describing endocasts assumes that the endocast provides an accurate impression of the brain, which is not the case (Jerison and Kielan-Jaworowska in preparation). As currently understood, an endocast is an impression of the brain, the meninges, and vessels that surround it (see e.g., Netter 1983; Altman and Bayer 1997, and many others).

Harry J. Jerison (HJJ, letter of 19 October 2003 to ZK-J) suggested to us that the region described in multituberculates as the "vermis" might be rather an impression of a superior cistern covering the midbrain and vermis. Netter (1983) referred to it as "cistern of the great cerebral vein". HJJ defined the superior cistern as follows: "It is a relatively large basin of the cerebrospinal fluid in the subarachnoid space in the region of the tectum mesencephali (anterior and posterior colliculi), extending from the anterior vermis of the cerebellum into the posterior space between the cerebral hemispheres. It communicates with ventricular system and cisterna magna. It is part of the system in which cerebrospinal fluid circulates in the brains of living mammals and was almost certainly similar in structure and function in fossil mammals. It must have been large enough in multituberculates to press on the internal table of the cranial cavity during development, to create the triangular bulge evident on the endocasts." HJJ also informed us that the only extant species showing a similar "enlarged vermis" known to him is the marsupial koala, in which the enlargement or bulge is due to the impression of the superior cistern, which made an appropriate impression on the skull. The midbrain (tectum mesencephali) is dramatically exposed in the koala brain but is covered on the endocast.

Following the above-discussed observations, we do not use the term vermis for the triangular bulge on multituberculate endocasts, and replace it by superior cistern. In relation to recognition of the superior cistern in endocasts of multituberculates and *Triconodon* (Simpson 1927), the previous terminology used for describing the endocasts of Mesozoic mammals should be changed.

Kielan-Jaworowska (1986) designated the multituberculate and eutriconodontan brains as cryptomesencephalic, and characterized them by the lack of midbrain exposure on the dorsal side. In this respect the multituberculate and eutriconodontan brains appeared to differ from brains of early therians (designated as eumesencephalic). Kielan-Jaworowska argued that in multituberculates the midbrain was obscured by an enlarged "vermis", rather than by the cerebral hemispheres, as in therians. The "vermis" was in direct contact with the paraflocculi and there were no obvious imprints of cerebellar hemispheres seen on the endocasts, as characteristic of therians. In the light of the present interpretation of multituberculate and eutriconodontan endocasts the terms cryptomesencephalic and eumesencephalic brains should be abandoned.

The question arises as to whether are we able to reconstruct the multituberculate brain on the basis of the structures seen on the endocasts. One can speculate that multituberculates possibly had brains of a structure generally similar to those of Cretaceous eutherian mammals, which is well reflected in their endocasts (e.g., Kielan-Jaworowska 1984, 1997). If so, the cerebellum in multituberculates was probably transversely elongated with a transverse anterior margin, in front of which the space between the diverging cerebral hemispheres was probably occupied by the midbrain, exposed on the dorsal side. There is, however, a difference. On endocasts of Cretaceous eutherian mammals, the vermis is delimited from the cerebellar hemispheres by the sigmoid sinus, lateral to which there is extensive development of the cerebellar hemisphere; lateral to that is a relatively small paraflocculus. In multituberculate endocasts the sigmoid sinus is situated more laterally (lateral to the wide superior cistern) than in eutherian endocasts, and lateral to it there is a large, transversely elongated paraflocculus. It is not clear whether the vermis occupied the whole width enclosed under the superior cistern: if so, it would be relatively wider than in eutherian mammals.

The new interpretation of multituberculate and *Triconodon* brains might have important phylogenetic implications. It may show that multituberculates, eutriconodontans, and

therians *sensu stricto* are more closely related to one another than hitherto believed (Kielan-Jaworowska et al. in press).

Endocast of *Kryptobaatar*

Introductory remarks.—Although *Kryptobaatar* is the most common mammalian genus in rocks of the Djadokhta Formation and Ukhaa Tolgod beds (Kielan-Jaworowska 1970, 1980, 1998; Rougier et al. 1996; Kielan-Jaworowska and Hurum 1997, 2001; Wible and Rougier 2000) and in the Bayan Mandahu Formation in China (Smith et al. 2001), its endocast has remained unknown.

Kielan-Jaworowska and Dashzeveg (1978) described a new multituberculate genus and species *Tugrigbaatar saichanensis*, based on a nearly complete skull with dentaries and fragments of the postcranial skeleton (GI PST 8-2) from Tögrög beds (equivalent of the Djadokhta Formation). Wible and Rougier (2000) claimed that *Tugrigbaatar saichanensis* Kielan-Jaworowska and Dashzeveg, 1978 is a junior synonym of *Kryptobaatar dashzevegi* Kielan-Jaworowska, 1970. Kielan-Jaworowska et al. (2000) accepted the congenerity, but not the conspecifity of the two taxa. Smith et al. (2001) described another species of *Kryptobaatar*, designated *K. mandahuensis* from the Bayan Mandahu Formation in China. Re-study of the individual variation among the specimens of *Kryptobaatar dashzevegi* housed in ZPAL and GI PST, and a comparison with the holotype of *Tugrigbaatar saichanensis* convinced Kielan-Jaworowska et al. (2003) that the differences between *T. saichanensis* and *K. dashzevegi* fall within the range of variation of *K. dashzevegi*. They agreed with Wible and Rougier (2000) that the two taxa are not only congeneric, but also conspecific, which we follow here.

Endocast from Tögrög (GI PST 8-2, Figs. 1, 2, 3B).—The endocast of GI PST 8-2, as originally preserved, was figured by Kielan-Jaworowska and Dashzeveg (1978: pl. 2: 1b); this specimen shows exposure of the partial endocast, including the superior cistern and cerebral hemispheres. After the paper by Kielan-Jaworowska and Dashzeveg (1978) was published, the first author (Z. K-J) removed a part of the cranial roof preserved in GI PST 8-2, as well as the bone surrounding the right paraflocculus and exposed nearly complete dorsal, lateral, and posterior aspects of the endocast (Figs. 1 and 2). Although the sand that filled the braincase after the death of the animal was extremely coarse, as it may be seen from the photographs published herein, details of the endocast are well visible.

The skull length of GI PST 8-2 has been estimated by Kielan-Jaworowska and Dashzeveg (1978) as about 30 mm; by comparison with the skull of ZPAL MgM-I/41, the length of which was estimated as 34 mm, we now think that 34 mm is also a more probable length for GI PST 8-2. The full length of the exposed endocast (which is slightly deformed) is about 17 mm, which is one half of the estimated skull length. The most characteristic feature of the endocast is the size of the impression of the olfactory bulbs, which are narrow and strongly elongated, about 6 mm long (which amounts to 35% of the endocranial cast length). The olfactory bulbs as a whole are narrow, their greatest width being at about one third of the length from the posterior; from that level they taper anteriorly and slightly posteriorly. In lateral view the olfactory bulbs are relatively shallow, especially anteriorly. The bulbs slightly diverge posteriorly and there is a single, median fusiform structure of unknown significance, interposed between the posterior part of the olfactory bulbs and the anterior part of the cerebral hemispheres. A similar, but a better preserved structure occurs in numerous endocasts of *Chulsanbaatar* (Kielan-Jaworowska 1983). Because of the distortion of the endocast (Fig. 1A), the cerebral part of this structure has been moved to the left with respect to the part lying at the end of the olfactory bulbs (but see reconstruction in Fig. 3B).

The cerebral hemispheres (measured in longitudinal projection) are about 8.8 mm long. They diverge slightly anteriorly, leaving a small, convex sub-triangular body (posterior part of the fusiform structure described above), which reaches the transverse furrow separating the cerebral hemispheres from the olfactory bulbs. Posteriorly the hemispheres diverge more strongly and embrace the bulbous roughly triangular structure that we call the superior cistern (the former "vermis"). The superior cistern is about 4 mm long in dorsal view and about 4.8 mm long in lateral view. Its maximum width is 5.3 mm. The casts of the transverse and sigmoid sinuses are partly preserved. A very large paraflocculus extends laterally (with slight posterior deviation) and ventrally as extension of the superior cistern (preserved on the endocast) and originate apparently from the vermis or other posterior cerebellar lobules, lying at the rear of the cerebral hemisphere.

Other endocasts of *Kryptobaatar* and individual variation.—In the collections of *K. dashzevegi* housed in ZPAL and GI PST, the endocast has been preserved only in GI PST 8-2. However, in ZPAL MgM-1/41 (see Kielan-Jaworowska and Gambaryan 1994: fig. 1), the endocranial cavity has been exposed, showing a very deep subarcuate fossa that extends into the base of the zygomatic arch.

Fragments of the endocast of *K. dashzevegi* have been figured by Wible and Rougier (2000: fig. 8, left stereo-photo) for PSS-MAE 101, but were not included in the right explanatory drawing to that figure. In this specimen the posterior part of the endocast is clearly seen, with the superior cistern deeply inserted between the cerebral hemispheres, which strongly diverge posteriorly. The size and proportions of the exposed part of the endocast are identical as in GI PST 8-2, figured here in Fig. 1.

The size of the olfactory bulbs is subject to individual variation in *Chulsanbaatar vulgaris* (Kielan-Jaworowska 1983: pl. 1, see also our Fig. 3A) and *Nemegtbaatar gobiensis* (Kielan-Jaworowska et al. 1986: fig. 18B and wax model in fig. 30). Therefore, it is not unlikely that the size of olfactory

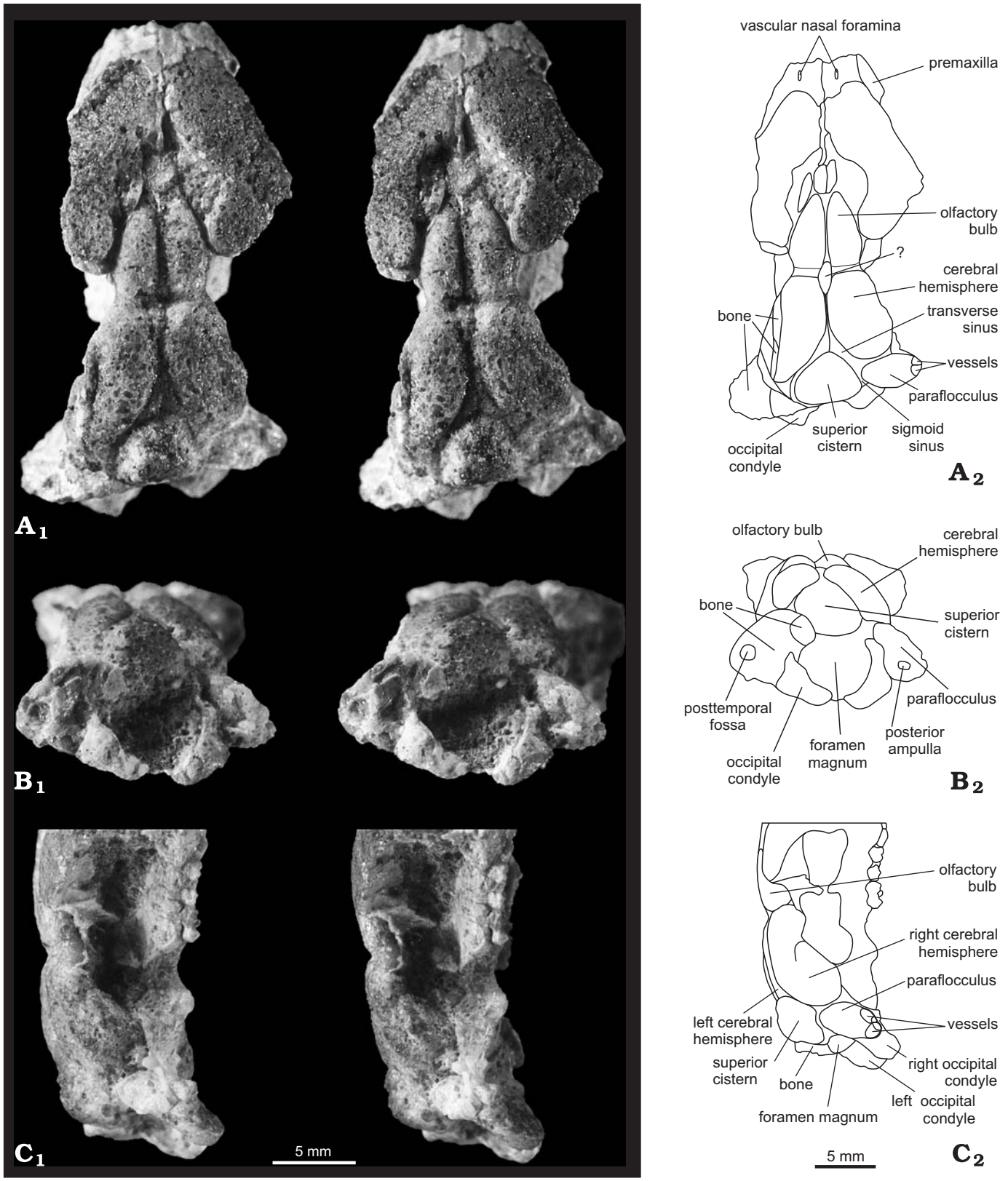

Fig. 1. *Kryptobaatar dashzevegi*, GI PST 8-2. **A**. Skull showing endocast in dorsal view. **B**. The same in posterior view. **C**. Posterior part of the same skull in right lateral view. A_1, B_1, C_1, stereo-photographs; A_2, B_2, C_2, explanatory drawings of the same, slightly reconstructed and reduced.

bulbs also varied in *Kryptobaatar dashzevegi*. Our conclusions about the olfactory bulbs and olfaction are based on the endocast, in which the bulbs may be significantly larger than the brain structures in this area.

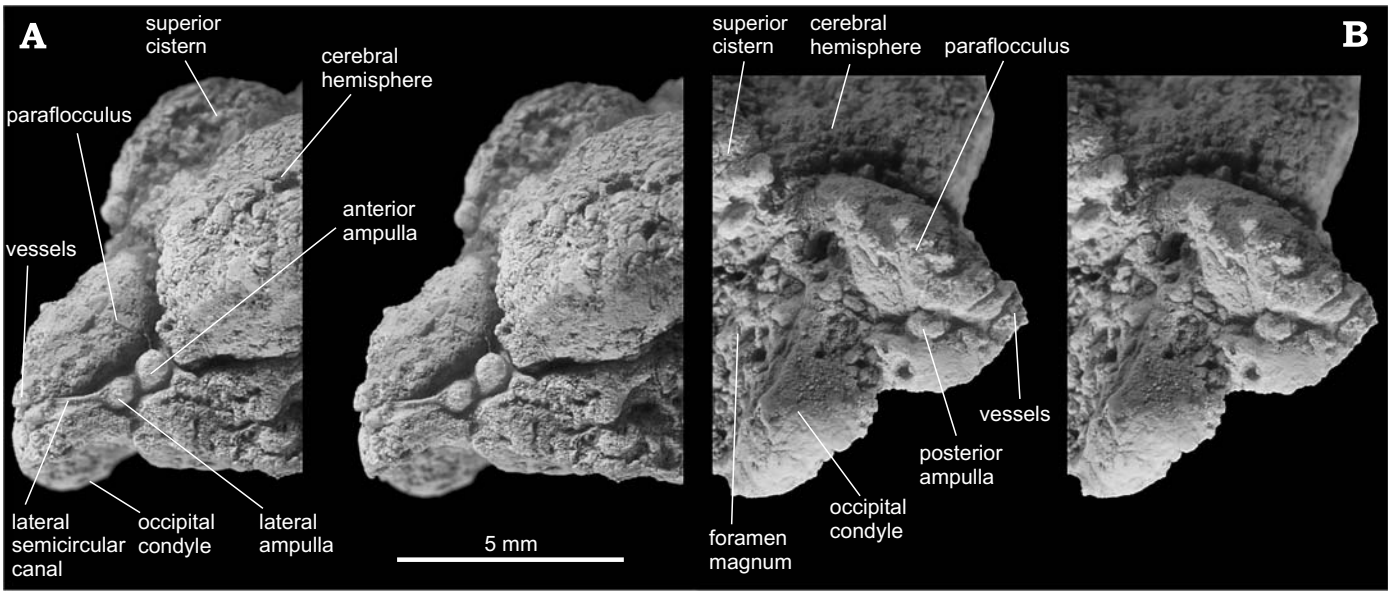

Fig. 2. *Kryptobaatar dashzevegi*, GI PST 8-2. **A**. Right parafloccculus in oblique ventro-lateral view, showing anterior ampulla, lateral ampulla, and lateral semicircular canal. **B**. The same in posterior view, showing posterior ampulla. Both stereo-photographs, coated with ammonium chloride.

Another specimen of *Kryptobaatar* that exposes the endocast belongs to *K. mandahuensis*. Smith et al. (2001: pl. 1: 1) figured the dorsal aspect of IMM 96BM-II/3, in which the posterior part of the cranial roof is damaged, showing a partial superior cistern and diverging cerebral hemispheres. In this specimen, again, the structure of the posterior part of the endocast appears similar to that in GI PST 8-2.

Inner ear fragments.—The multituberculate inner ear is well known, due mostly to the meticulous work of Fox and Meng (1997, see also references to earlier literature therein), based on CT-scan, X-radiographic, and SEM study of unidentified Bug Creek petrosals, and Hurum (1998) based on serial sections and enlarged models of *Nemegtbaatar* and *Chulsanbaatar*.

Our contribution to the knowledge on inner ear structure is modest and concerns recording the preservation of fragments of semicircular canals and ampullae in GI PST 8-2 around the right parafloccculus (Figs. 1B, C and 2). In front of the middle part of the parafloccculus two osseous ampullae adhering to each other are clearly seen (Fig. 2A). The more proximal ampulla (of the anterior semicircular canal) adheres to the postero-lateral end of the cerebral hemisphere. The anterior semicircular canal has not been preserved; it extended in a groove between the posterior end of the cerebral hemisphere and parafloccculus, as in *Chulsanbaatar* (Hurum 1998: fig. 15). The more distal ampulla (of the lateral semicircular canal) is placed postero-laterally with respect to the ampulla of the anterior semicircular canal. A part of the lateral semicircular canal has been preserved, extending from the ampulla postero-laterally, above the lateral part of the parafloccculus. The ampulla of the posterior semicircular canal has also been preserved and is seen in the posterior view of the endocast (Figs. 1C, 2B) below the parafloccculus, but the canal has not been found.

Hurum (1998) based his studies upon the model of the inner ear prepared by Kielan-Jaworowska et al. (1986) during their study on serial sectioning of the skull of *Nemegtbaatar*. On the basis of the model, Hurum (1998: figs. 6 and 7) made a reconstruction of the inner ear of *Nemegtbaatar* (fig. 17B in his paper). In that reconstruction the ampullae are less sharply delimited from the canals than, for example, in the extant guinea pig (see Hurum 1998: fig. 17D). The ampullae preserved in GI PST 8-2 and the whole system of semicircular canals, as inferred from the preserved fragments resemble the reconstruction of multituberculate inner ear made by Fox and Meng (1997: fig. 2C).

Comparison with endocasts of other multituberculates.—The endocast of *Kryptobaatar dashzevegi* (Figs. 1, 2, 3B) differs from those of other multituberculates in having relatively longer olfactory bulbs. In *Chulsanbaatar* (Fig. 3A) and *Nemegtbaatar* Kielan-Jaworowska et al. (1986: fig. 20a) the olfactory bulbs are shorter, and their length varies at about 1/4 of the total endocast length. The olfactory bulbs appear to be relatively narrower in *K. dashzevegi* than in *Chulsanbaatar* and *Nemegtbaatar*. The shape of the olfactory bulbs in *K. dashzevegi* is probably most similar to that of *Ptilodus montanus* (USNM 9710) figured by Krause and Kielan-Jaworowska (1993: pl. 1: 1), although the greatest width of the bulbs in *K. dashzevegi* is situated more posteriorly.

Another difference with multituberculate endocasts of other taxa concerns the shape and size of the paraflocculi, which, however, may not fill completely the volume of the subarcuate fossa (Sánchez-Villagra 2002). In *Chulsanbaatar*, *Nemegtbaatar*, and apparently also in *Ptilodus* (if Simpson's 1937 reconstruction is in this respect correct) the

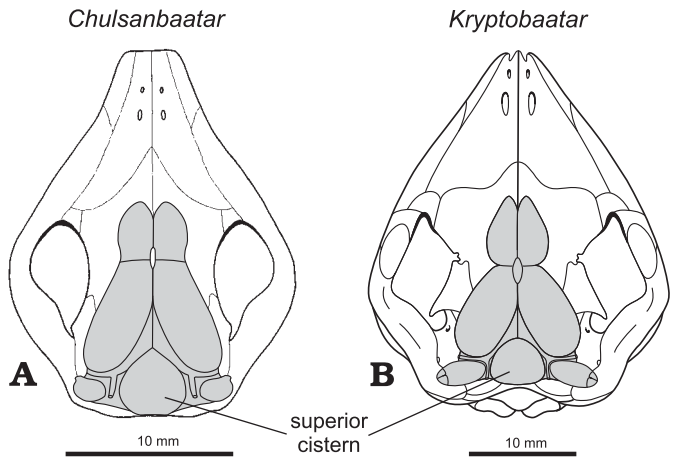

Fig. 3. Reconstruction of two Late Cretaceous multituberculate endocasts superimposed on the outlines of the skull (rendered to the same length) in dorsal view. A. *Chulsanbaatar vulgaris*. **B**. *Kryptobaatar dashzevegi*. A, modified from Kielan-Jaworowska et al. (1986); B, original. The outline of the skull in B, based on reconstruction of Wible and Rougier (2000: fig. 30), and data from the collection of *K. dashzevegi*, housed in ZPAL; the nasal vascular foramina are based in the holotype specimen ZPAL MgM-I/21.

paraflocculi are rounded in all the views (ball-shaped). In *K. dashzevegi*, in contrast, the paraflocculus is narrower longitudinally, extending laterally (with slight posterior deviation) and ventrally. The paraflocculus in GI PST 8-2 shows division into larger proximal and smaller distal parts; the distal part might correspond to the vessels referred to for *Nemegtbaatar* (Kielan-Jaworowska et al. 1986: fig. 32) as "posttemporal recess vessels" (= arteria diploetica magna, see Rougier et al. 1992). However, as the sediment that filled the subarcuate fossa in GI PST 8-2 is coarse-grained, the reconstruction of these vessels was not possible, and we refer to them in Figs. 1 and 2 simply as vessels. In living mammals the flocculus-paraflocculus system is related to oculomotor and other sensorimotor coordination, and correlated with this function, it is involved in the control of such coordination by higher mental processes (Altman and Bayer 1997).

Encephalization quotient

EQ of *Kryptobaatar* based on Jerison's equation.—Jerison (1973) proposed an equation for estimating EQ in fossil mammals, which was subsequently modified by Kielan-Jaworowska (1983), Thewissen and Gingerich (1989), and Krause and Kielan-Jaworowska (1993, see discussion in that paper for details). Jerison (1973) used the coefficient 0.050 (adopted for heavily built mammals) for estimation of body mass in multituberculates. Kielan-Jaworowska (1983) questioned this and used the coefficient 0.025, assuming that *Kryptobaatar* was not fossorial (as subsequently demonstrated by Kielan-Jaworowska and Gambaryan 1994) and therefore regarded the coefficient for small, lightly built mammals as appropriate. Although the multituberculate skull, which is compressed dorso-ventrally rather than laterally as in therian mammals, appears more robust than that of small therians of similar size, the multituberculate postcranial skeleton (Granger and Simpson 1929; Krause and Jenkins 1983; Kielan-Jaworowska and Gambaryan 1994; Sereno and McKenna 1995; Gambaryan and Kielan-Jaworowska 1997; Kielan-Jaworowska 1998) appears to be of comparable robustness to those of small eutherian mammals of similar size. An exception are the fossorial multituberculates (e.g., Miao 1988; Kielan-Jaworowska and Qi 1990; Gambaryan and Kielan-Jaworowska 1997), in which the postcranial skeleton is decidedly robust. Table 1 gives the estimation of the encephalization quotient (EQ) in *K. dashzevegi*, using the modified Jerison equation:

$$EQ = \frac{E}{0.055 Wt^{0.74}} \qquad (1)$$

in which E is brain volume in milliliters and Wt is body weight in grams.

Table 1. Endocast volume, body size and encephalization quotient in *Kryptobaatar dashzevegi*, based on modified Jerison equation.

Computations (length in cm, volumes in ml, weights in g)	Olfactory bulbs	Endocast exclusive of olfactory bulbs	Total endocast
Endocast volume			
Mean width (w)	0.47	1.05	
Mean height (h)	0.38	0.84	
Length (l)	0.6	1.1	1.7
Estimated volume ($E = 1/4\pi\, l\, w\, h$)	0.084	0.76	0.84
Body size			
Skull length (S)		3.40	
Body length (L)		13.60	
Body weight ($Wt = 0.025\, L^3$)		62.9	
Encephalization quotient $EQ = \frac{E}{0.055 Wt^{0.74}}$ (1)		0.71	

EQ of *Kryptobaatar* based on M1–M2 length measurements.—The relationship between tooth size and body size has been studied in many mammals, e.g., primates (Gingerich 1974; Kay 1975; Wood 1979; Fleagle 1985), insectivores (Gingerich and Smith 1984; Thewissen and Gingerich 1989), carnivores (Van Valkenburgh 1990), ungulates (Janis 1990), and marsupials (Gordon 2003). Tooth size has also been used to predict the body masses of extinct mammals (Gingerich et al. 1982; Bloch et al. 1998; Wood and Clemens 2001). McDermott et al. (2002) proposed a method of estimating body mass in multituberculates based upon the length of upper molars M1 and M2. They derived a new equation for predicting body mass in rodents using tooth row length (TRL). These authors concluded that the M1–M2 length in multituberculates is comparable to TRL in rodents. In using this methodology, we averaged the reported M1 and M2

lengths from Table 1 in Kielan-Jaworowska et al. (2003) and added the two averages together to produce one representative M1–M2 length for *Kryptobaatar*. We calculated the body mass estimate for *Kryptobaatar* from the M1 and M2 measurements using, equation (2) the derived equation from McDermott et al. (2002).

$$\log(BM) = 2.87 \times \log(TRL) - 0.36 \qquad (2)$$

in which BM is body mass in grams and TRL is tooth row length in millimeters. For multituberculates, the upper molar M1 and M2 length (M1–M2) is substituted for TRL in this equation. An EQ of 1.06 was calculated from this estimated body mass using Jerison's equation (1). The estimated body mass and EQ are listed in Table 2. Prediction limits (95%) were calculated as described in Sokal and Rohlf (1995).

Table 2. Measurements, regression equations, and body mass estimates of *Kryptobaatar dashzevegi* from upper molar length measurements.

Upper molar length measurements in mm and weights in g	
Average upper molar M1 length	2.73
Average upper molar M2 length	1.96
Average M1–M2 length	4.68
Estimated body mass	36.6
95% prediction upper limit	88.3
95% prediction lower limit	15.2
Encephalization Quotient	1.06

EQ of *Kryptobaatar* based on humerus, radius, ulna, femur, and tibia measurements.—Body mass predictions have also been made from long bone measurements using bivariate linear regression analysis and multiple regression analysis to determine allometric relationships based on body mass, bone length, and diameter (Alexander et al. 1979; Gingerich 1990; Martin 1992; Christiansen, 1999; Saysette 1999; and Reynolds 2002). These predictions are calculated from the analysis of different long bone measurements on the log-transform of $Y=aX^b$ where Y is the bone length or diameter and X is the body mass.

Since many of the long bones for *Kryptobaatar* are not known, or are incompletely preserved, we developed a series of regression equations to provide body mass estimates for *Kryptobaatar* based upon the long bone material available for this species. We based our predictions on long bone measurements of 32 individuals from 14 extant rodent species (see Table 3). According to Kielan-Jaworowska and Gambaryan (1994, *contra* Sereno and McKenna 1995, and Sereno in press), *Kryptobaatar* had abducted limbs (i.e., sprawling stance) similar to those of modern monotremes. We did not use monotremes in creating our body mass prediction model, as all three species of modern monotremes have a much more heavily built skeleton and are much larger in size (Griffiths 1968, 1978) than the Cretaceous multituberculates studied by us. As stated in a previous section, the multituberculate postcranial skeleton (Granger and Simpson 1929; Krause and Jenkins 1983; Kielan-Jaworowska and Gambaryan 1994; Sereno and McKenna 1995; Gambaryan and Kielan-Jaworowska 1997; Kielan-Jaworowska 1998) is similar in robustness to those of small eutherian mammals of similar size. Therefore, we chose rodents as the ecological equivalent of multituberculates for the prediction of body mass for *Kryptobaatar*. As well as being similar in structure and size to *Kryptobaatar*, all rodent species used for our regression models have a body mass that is less than 3.5 kg and also have a known brain mass (Pilleri 1959). These species are listed in the Appendix.

Maximum length and midshaft diameter from both the right and left bones were averaged for a single length or diameter variable. We measured the midshaft diameters in two planes: first in the plane of the tibial crest[1] and second perpendicular to the tibial crest. Whenever possible, we measured both a male and a female for each species and used sex-specific masses. Where available we used the actual body mass of each specimen, otherwise we calculated a mean mass for each species (Bonin 1937; Crile and Quiring 1940; Pilleri 1959; Eisenberg 1981; Damuth and MacFadden 1990; Silva and Downing 1995).

Table 3. Extant rodent species used for body mass estimation.

Family	Species (N)	
Sciuridae	*Sciurus vulgaris* (1) *Sciurus carolinensis* (2) *Ratufa indica* (2)	*Protoxerus stangeri* (2) *Spermophilus tridecemlineatus* (2) *Spermophilus citellus* (2)
Anomaluridae	*Anomalurus pusillus* (2)	
Hystricidae	*Atherurus africanus* (2)	
Caviidae	*Cavia porcellus* (3)	
Dasyproctidae	*Dasyprocta leporina* (4)	
Chinchillidae	*Chinchilla lanigera* (4)	*Chinchilla brevicaudata* (2)
Cricetidae	*Ondatra zibethicus* (2)	
Heteromyidae	*Peromyscus maniculatus* (2)	

For estimation of body mass we employed the allometric equation:

$$Y = kX^a \qquad (3)$$

in which Y is the body mass, X is the bone length/diameter measurement, k is the proportionality coefficient (or the Y-intercept) and a is the slope of the regression line of the log transform (Jerison 1973; Schmidt-Nielsen 1984; Zar 1999). We used the reported length measurements from Sereno and McKenna (1995) along with the hind limb lengths for ZPAL MgM-I/41 in the first regression calculation. The step-wise regression of all variables measured for *Kryptobaatar* showed the diameter of the tibia in the plane through the tibial crest to be the largest contributor to the estimation of body mass.

[1] The term tibial crest (*crista tibiae*), which we use, has been replaced in *Nomina Anatomica Veterinaria* (see Schaller 1992) by cranial border (*margo cranialis*).

Table 4. Measurements, regression equations, and body mass estimates of *Kryptobaatar dashzevegi* from postcranial measurements.

Postcranial measurements in mm and weights in g			
From Sereno and McKenna (1995)			
Humerus length	15.7		
Radius length	12.0		
Ulna length	16.0		
From ZPAL MgM-I/41			
Right femur length	25.0		
Right femur diameter (plane through tibial crest)	2.4		
Left femur length	24.3		
Left femur diameter (plane perpendicular to tibial crest)	2.8		
Right tibia length	18.8		
Right tibia diameter (plane through tibial crest)	1.1		
Right tibia diameter (plane perpendicular to tibial crest)	2.5		
Body mass equations	Predicted body mass	95% Prediction Limits	EQ
(3a) $Wt = 720.4 (X_1^{3.778} * X_2^{-1.265} * X_3^{1.415} * X_4^{-2.611} * X_5^{-0.383} * X_{61.454} * X_7^{1.214} * X_8^{0.139} * X_9^{-1.507})$ $r = 0.942$	32.6	5.1 – 208.6	0.76
(3b) $Wt = 0.078(X_1^{6.248} * X_2^{-5.814} * X_3^{3.816} * X_4^{-4.776} * X_5^{2.727})$ $r = 0.930$	35.2	13.8 – 202.6	1.04
(3c) $Wt = 1.622(X_4^{2.311} * X_5^{-1.548} * X_6^{0.735} * X_7^{2.270} * X_8^{1.154} * X_9^{-2.630})$ $r = 0.919$	56.2	3.0 – 1050.2	0.75
($3d_1$) $Wt = 0.062(X_1^{2.451})$ $r = 0.886$	52.9	4.9 – 189.1	0.78
($3d_2$) $Wt = 0.066(X_2^{2.470})$ $r = 0.813$	30.6	7.1 – 197.8	1.15
($3d_3$) $Wt = 0.037(X_3^{2.500})$ $r = 0.841$	37.4	15.8 – 430.5	1.00
($3d_4$) $Wt = 0.032(X_4^{2.454})$ $r = 0.828$	82.3	6.1 – 294.8	0.57
($3d_5$) $Wt = 0.061(X_5^{2.230})$ $r = 0.762$	42.2	36.1 – 695.7	0.91
($3d_6$) $Wt = 22.59(X_6^{2.224})$ $r = 0.857$	158.3	39.9 – 661.9	0.36
($3d_7$) $Wt = 18.20(X_7^{2.218})$ $r = 0.872$	178.6	9.8 – 252.6	0.33
($3d_8$) $Wt = 41.78(X_8^{1.801})$ $r = 0.832$	49.6	59.3 – 1213.2	0.82
($3d_9$) $Wt = 40.55(X_9^{2.061})$ $r = 0.836$	268.0	2.8 – 869.9	0.25

Wt = body mass, X_1 = humerus length, X_2 = radius length, X_3 = ulna length, X_4 = femur length, X_5 = tibia length, X_6 = femur anterior-posterior diameter, X_7 = femur transverse diameter, X_8 = tibia anterior-posterior diameter, X_9 = tibia transverse diameter

We produced a multivariable regression equation (3a) based on the lengths of the humerus, radius, ulna, and the lengths and midshaft diameters of the femur and tibia. We also formulated another multivariable regression equation (3b) based solely on the lengths of the humerus, radius, ulna, femur and tibia as well as a multivariable regression equation (3c) generated from the length and diameter measurements of the femur and tibia only. We further derived simple regression equations for each length variable and diameter variable ($3d_1$, $3d_2$, $3d_3$, $3d_4$, $3d_5$, $3d_6$, $3d_7$, $3d_8$, and $3d_9$). The regression equations and the resulting predicted body masses are shown in Table 4. Although the hind limbs of *K. dashzevegi* (ZPAL MgM-I/41, see Kielan-Jaworowska and Gambaryan 1994: fig. 2) are nearly complete, the femur and tibia are the only long bones of which the all the measurements could be taken. The complete humerus, radius, and ulna of *Kryptobaatar* have been preserved in specimen PSS-MAE-103, referred to originally by Sereno and McKenna (1995) to *Bulganbaatar nemegtbaataroides*, but regarded by Sereno (in press) as belonging to *Kryptobaatar dashzevegi*. The humerus PSS-MAE-101, figured by Dashzeveg et al. (1995: fig. 3a, referred to as "compare *Chulsanbaatar vulgaris*") lacks the

humeral head. The humerus from Ukhaa Tolgod GI5/302, figured by Kielan-Jaworowska (1998: figs. 1, 2) is almost complete but lacks the compact layer of the bone in the middle of the shaft, and therefore the diameter of the shaft could not be measured. While lengths were reported for the humerus, radius, and ulna in Sereno and McKenna (1995), the midshaft diameters were not recorded. Thus, the regression of the midshaft diameters could not be completed for these bones.

From the same 32 rodent specimens used to create the body mass regression equations, we derived a brain mass prediction equation using known body and brain masses and simple linear regression (Bonin 1937; Crile and Quiring 1940; Pilleri 1959; Eisenberg 1981; Damuth and MacFadden 1990; Silva and Downing 1995). True brain masses were averaged to provide one mean brain mass variable per species. Body masses were determined as described above. The resulting equation is:

$$Y = 0.070(X^{0.697}) \quad (4)$$

in which Y is the brain mass and X is the body weight (r = 0.909). We determined the predicted brain mass from each body mass calculated from our derived equations (3a, 3b, 3c, and $3d_{1–9}$). Equation (4) predicts brain weight in grams, but brain volume is needed to calculate EQ. Therefore, we used the specific density of water, 1.036 g/cm^3, to convert each predicted brain weight in grams to a volume in milliliters (Hopkins and Marino 2000) for comparison to the measured endocast volume for *Kryptobaatar dashzevegi*. We used the equation:

$$E = 0.25\pi lwh \quad (5)$$

in which E is the estimated endocast volume and l, w, and h are the length, width and height of the endocast, to determine the estimated volume of the total endocast for *Kryptobaatar dashzevegi*, which is 0.84 ml.

We then calculated the encephalization quotient (EQ) for each predicted brain volume of *Kryptobaatar dashzevegi* using the equation:

$$EQ = \frac{E}{V} \quad (6)$$

in which E is the estimated volume of the endocast, 0.84 ml, and V is the predicted brain weight from the regression equation converted into milliliters, 1.186 ml.

The resulting EQ's are shown in Table 4.

Discussion of body mass prediction methods and resulting EQ values.—The predicted body mass using Jerison's method was 62.9 g and the resulting EQ was 0.71. The predicted body mass using McDermott et al.'s method (2) was 36.6 g and the resulting EQ was 1.06. Body masses predicted from our derived equations (3a, 3b, 3c, $3d_{1–9}$) range from 30.6 to 268.0 g with a mean weight of 85.3 g. The EQs predicted from these body masses range from 0.25 to 1.15, with a mean EQ of 0.73. The single variable regression equations we generated using only one measurement from a long bone resulted in a wide range of mass predictions, 30.6 to 268.0 g, compared to the multiple regression equations we generated using multiple measurements or multiple bones, 32.6 to 56.2 g. The predicted mass from McDermott et al.'s tooth measurement regression, 36.6 g, is comparable to the low range of mass predictions we produced with our derived equations (3a, 3b, 3c, $3d_{1–9}$) and, therefore, the resulting EQ from McDermott et al.'s mass prediction, 1.06, was in the high range of our calculated EQs. The mean of our mass predictions, 85.3 g, was similar to the predicted mass from Jerison's single variable regression of body length, 62.9 g, and the mean EQ from our predictions was very similar to the EQ calculated from Jerison's method (1), 0.73 and 0.71 respectively.

Conclusions and speculations

The new interpretation of multituberculate and eutriconodontan endocasts presented herein suggests that it appears possible that the differences between the brain structure of multituberculates, eutriconodontans on one side, and early eutherian and marsupial mammals, on the other, was smaller than previously thought. It seems possible (but not proven) than in multituberculate and eutriconodontan brains the midbrain was exposed dorsally, as in the endocasts of Cretaceous eutherian mammals, and in brains of primitive extant placentals and marsupials. The differences between multituberculates + eutriconodontans and early therians *sensu stricto*, as inferred from their endocasts, concern cranial vasculature, but apparently not the general design of the brain.

The encephalization quotient of *Kryptobaatar dashzevegi* calculated by us (upon estimating the body mass from the skull size) is 0.71 (Table 1), and using the mean from our new equation (6) is 0.73. The EQ value of 1.06 obtained using McDermott et al.'s (2002) method appears to be an overestimate. The value of 0.71 is higher than that obtained for the two other multituberculates for which EQ was calculated. The EQ for *Ptilodus* obtained by Krause and Kielan-Jaworowska (1993), including the olfactory bulbs, is 0.62, while excluding the olfactory bulbs is 0.55. The EQ calculated by Kielan-Jaworowska (1983, 1986) for *Chulsanbaatar vulgaris* (including the olfactory bulbs) is 0.54–0.56. The relatively high EQ calculated for *Kryptobaatar* is similar to that obtained by Kielan-Jaworowska (1984) for the Late Cretaceous eutherian mammal *Zalambdalestes*, which is 0.70.

From the size of the olfactory bulbs on the endocasts, we judge that the main multituberculate sense was olfaction, as it is for most extant mammals. Also the large ear region, as inferred from the structure of the basicranium, implies acute hearing. Finally very large paraflocculi suggest well-developed sensorimotor adaptations, in particular coordinated movements. The strong development of all these senses indicates a nocturnal mode of life of multituberculates, as suggested for all Mesozoic mammals by Jerison (1973) and many others.

Kryptobaatar was a dominant mammalian taxon during the time of deposition of the Djadokhta and Bayan Mandahu formations (?early Campanian), and the Ukhaa Tolgod beds. This multituberculate has also recently been found (Kielan-Jaworowska et al. 2003) in the Hermiin Tsav beds, which are an equivalent of the ?late Campanian Baruungoyot Formation. It follows that *Kryptobaatar* might have existed in the region which is now the Gobi Desert during the whole Campanian (for about 18 million years). It remains an open question whether the long dominance of *Kryptobaatar* in the Late Cretaceous Gobi Desert mammalian communities might have been related to its relatively high EQ.

Acknowledgements

During the work on this paper we greatly benefited from advice and discussion with numerous colleagues and friends who read the early drafts of the manuscript of this paper, provided comments and offered assistance in various ways. Prime among them were: Harry Jerison, whose experience and knowledge in neurology and paleoneurology and continuous advise were of an enormous assistance to us; J.G.M. Thewissen, who offered his knowledge and insights of mammalian morphology in the design and analysis of the rodent regression equations; Demberlyin Dashzeveg, who allowed us to use in this study the specimen of *Kryptobaatar dashzevegi*, found by him and housed in GI PST collection. John R. Wible and John Hunter reviewed the earlier version of the paper and offered very important comments, Christine M. Janis and Krzysztof Turlejski discussed several questions with us; Paul Sereno sent us the MS of his paper in press and allowed us to cite it. TEL thanks the authorities of the American Museum of Natural History, the Carnegie Museum of Natural History, the National Museum of Natural History (Smithsonian Institution), and the University of Michigan Museum of Zoology for permission to study collections of modern rodents. The photographs published here were been taken by Marian Dziewiński, while Andrzej Kaim processed them and made the accompanying computer drawings; the drawing published as Fig. 3 has been made by Aleksandra Hołda (all from the Institute of Paleobiology in Warsaw). To all these persons and institutions we express our sincere thanks and gratitude.

References

Alexander, R.McN., Jayes, A.S., Maloiy, G.M.O., and Wathuta, E.M. 1979. Allometry of the limb bones of mammals from shrews (*Sorex*) to elephant (*Loxodonta*). *Journal of Zoology, London* 189: 305–314.

Altman, J. and Bayer, S. A. 1997. *Development of the Cerebellar System: Its Relation to Its Evolution, Structure, and Functions.* CRC Press, Boca Raton, Florida, New York, viii + 783pp.

Bauchot, R. and Stephan, H. 1967. Encéphales et moulages endocraniens de quelques insectivores et primates endocraniens. In: Problemes Actuels de Paléontologie (Evolution des Véertebrés). Colloques Internationaux du CNRS 163. Paris Editions du CNRS: 575–586.

Bloch, J.I., Rose, K.D., and Gingerich, P.D. 1998. New species of *Batodonoides* (Lipotyphla, Geolabididae) from the Early Eocene of Wyoming: Smallest known mammal? *Journal of Mammalogy* 79: 804–827.

Bonin, G., von, 1937. Brain-weight and body-weight of mammals. *Journal of General Psychology* 16: 379–389.

Christiansen, P. 1999. Long bone scaling and limb posture in non-avian theropods; evidence for differential allometry. *Journal of Vertebrate Paleontology* 19 (4): 666–680.

Crile, G. and Quiring, D.P. 1940. A record of the body weight and certain organ and gland weights of 3690 animals. *The Ohio Journal of Science* 40 (5): 219–259.

Damuth, J. and MacFadden, B.J. 1990. *Body Size in Mammalian Paleobiology: Estimation and Biological Implications*. 397 pp. Cambridge University Press, Cambridge.

Dashzeveg, D., Novacek, M.J., Norell, M.A., Clark, J.M., Chiappe L.M., Davidson, A., McKenna, M.C., Dingus, L., Swisher, C., and Altangerel, P. 1995. Extraordinary preservation in a new vertebrate assemblage from the Late Cretaceous of Mongolia. *Nature* 374: 446–449.

Eisenberg, J.F. 1981. *The Mammalian Radiations: An analysis of Trends in Evolution, Adaptation, and Behavior*. 610 pp. The University of Chicago Press, Chicago.

Fleagle, J.G. 1985. Size and adaptation in primates. *In*: W.L. Jungers (ed.), *Size and Scaling in Primate Biology*, 1–19. Plenum Press. New York.

Fox, R.C. and Meng, J. 1997. An X-radiographic and SEM study of the osseous inner ear of multituberculates and monotremes (Mammalia): implications for mammalian phylogeny and evolution of hearing. *Zoological Journal of the Linnean Society* 121: 249–291.

Gambaryan, P.P. and Kielan-Jaworowska, Z. 1997. Sprawling versus parasagittal stance in multituberculate mammals. *Acta Palaeontologica Polonica* 42: 13–44.

Gingerich, P.D. 1974. Dental function in the Paleocene primate *Plesiadapis. In*: R.D. Martin, G.A. Doyle, and A.C. Walker (eds.), *Prosimian Biology*, 531–541, University of Pittsburgh Press, Pittsburgh.

Gingerich, P.D. 1990. Prediction of body size in mammalian species from long bones lengths and diameters. *Contributions from the Museum of Paleontology, the University of Michigan* 28: 79–92.

Gingerich, P.D. and Smith, B.H. 1984. Allometric scaling in the dentition of primates and insectivores. *In*: W.L. Jungers (ed.), *Size and Scaling in Primate Biology*, 257–272. Plenum Press, New York.

Gingerich, P.D., Smith, B.H., and Rosenberg, K. 1982. Allometric scaling in the dentition of primates and prediction of body weight from tooth size in fossils. *American Journal of Physical Anthropology* 58: 81–100.

Gordon, C.L. 2003. A first look at estimating body size in dentally conservative marsupials. *Journal of Mammalian Evolution* 10 (1/2): 1–21.

Granger, W. and Simpson, G.G. 1929. A revision of the Tertiary Multituberculata. *Bulletin of the American Museum of Natural History* 56: 601–676.

Griffiths, M. 1968. *Echidnas*. 282 pp. Pergamon Press, London.

Griffiths, M. 1978. *The Biology of Monotremes.* 367 pp. Academic Press, New York.

Hahn, G. 1969. Beiträge zur Fauna der Grube Guimarota Nr. 3. Die Multituberculata. *Palaeontographica A* 133: 1–100.

Hopkins, W.D. and Marino, L. 2000. Asymmetries in cerebral width in nonhuman primate brains as revealed by magnetic resonance imaging (MRI). *Neuropsychologia* 38 (4): 493–499.

Hurum, J.H. 1998. The inner ear of two Late Cretaceous multituberculate mammals, and its implications for multituberculate hearing. *Journal of Mammalian Evolution* 5: 65–94.

Janis, C.M. 1990. Correlation of cranial and dental variables with body size in ungulates and macropodids. *In*: J. Damuth and B.J. MacFadden (eds.), *Body Size in Mammalian Paleobiology*, 255–299. Cambridge University Press, Cambridge, England.

Jerison, H.J. 1973. *Evolution of Brain and Intelligence*. 482 pp. Academic Press, New York.

Kay, R.F. 1975. The functional adaptations of primate molar teeth. *Journal of Physical Anthropology* 43: 195–216.

Kielan-Jaworowska, Z. 1970. New Upper Cretaceous multituberculate genera from Bayn Dzak, Gobi Desert. *In*: Z. Kielan-Jaworowska (ed.), Results of the Polish-Mongolian Palaeontological Expeditions, pt. II. *Palaeontologia Polonica* 21: 35–49.

Kielan-Jaworowska, Z. 1974. Multituberculate succession in the Late Cretaceous of the Gobi Desert (Mongolia). *In:* Z. Kielan-Jaworowska (ed.),

Results of the Polish-Mongolian Palaeontological Expeditions, pt. V. *Palaeontologia Polonica* 30: 23–44.

Kielan-Jaworowska, Z. 1980. Absence of ptilodontoidean multituberculates from Asia and its palaeogeographic implications. *Lethaia* 13: 169–173.

Kielan-Jaworowska, Z. 1983. Multituberculate endocasts. *Palaeovertebrata* 13: 1–12.

Kielan-Jaworowska, Z. 1984. Evolution of the therian mammals in the Late Cretaceous of Asia. Part VI. Endocasts of eutherian mammals. *Palaeontologia Polonica* 46: 157–171.

Kielan-Jaworowska, Z. 1986. Brain evolution in Mesozoic mammals. *Contributions to Geology, University of Wyoming Special Paper* 3: 21–34.

Kielan-Jaworowska, Z. 1997. Characters of multituberculates neglected in phylogenetic analyses of early mammals. *Lethaia* 29: 249–266.

Kielan-Jaworowska, Z. 1998. Humeral torsion in multituberculate mammals. *Acta Palaeontologica Polonica* 43: 131–134.

Kielan-Jaworowska, Z. and Dashzeveg, D. 1978. New Late Cretaceous locality in Mongolia and a description of a new multituberculate. *Acta Palaeontologica Polonica* 23: 115–130.

Kielan-Jaworowska, Z. and Gambaryan, P.P. 1994. Postcranial anatomy and habits of Asian multituberculate mammals. *Fossils and Strata* 36: 1–92.

Kielan-Jaworowska, Z. and Hurum, J.H. 1997. Djadochtatheria a new suborder of multituberculate mammals. *Acta Palaeontologica Polonica* 42: 201–242.

Kielan-Jaworowska, Z. and Hurum, J.H. 2001. Phylogeny and systematics of multituberculate mammals. *Palaeontology* 44: 389–429.

Kielan-Jaworowska, Z. and Qi, T. 1990. Fossorial adaptations of a taeniolabidoid multituberculate mammal from the Eocene of China. *Vertebrata PalAsiatica* 28: 83–94.

Kielan-Jaworowska, Z., Cifelli, R.L., and Luo, Z-X. (in press). *Mammals from the Age of Dinosaurs: Origins, Evolution, and Structure*. Columbia University Press, New York.

Kielan-Jaworowska, Z., Hurum, J.H., and Badamgarav, D. 2003. An extended range of the multituberculate *Kryptobaatar* and the distribution of mammals in the Upper Cretaceous of the Gobi Desert. *Acta Palaeontologica Polonica* 48 (2): 273–278.

Kielan-Jaworowska, Z., Novacek, M.J., Trofimov, B.A., and Dashzeveg, D. 2000. Mammals from the Mesozoic of Mongolia. *In*: M.J. Benton, M.A. Shishkin, D.M. Unwin, and E.N. Kurochkin (eds.), *The Age of Dinosaurs in Russia and Mongolia*, 573–626. Cambridge University Press, Cambridge.

Kielan-Jaworowska, Z., Presley, R., and Poplin, C. 1986. The cranial vascular system in taeniolabidoid multituberculate mammals. *Philosophical Transactions of the Royal Society of London B* 313: 525–602.

Krause, W.D. and Jenkins, F.A., Jr. 1983. The postcranial skeleton of North American multituberculates. *Bulletin of the Museum of Comparative Zoology* 150: 199–246.

Krause, W.D. and Kielan-Jaworowska, Z. 1993. The endocast and encephalization quotient of *Ptilodus* (Multituberculata, Mammalia). *Palaeovertebrata* 22: 99–112.

Martin, R.A. 1992. Generic species richness and body mass in North American mammals; support for the inverse relationship of body size and speciation rate. *Historical Biology* 6 (3): 73–90.

McDermott, B., Hunter, R.J., and Alroy, J. 2002. Estimating body mass of multituberculate mammals. *Journal of Vertebrate Paleontology* 22 (Supplement to No. 3), Abstracts: 86A.

Miao, D. 1988. Skull morphology of *Lambdopsalis bulla* (Mammalia, Multituberculata) and its implications to mammalian evolution. *Contributions to Geology, University of Wyoming, Special Paper* 4: 1–104.

Netter, Frank, H. 1983. *The Ciba Collection of Medical Illustrations, Volume 1, Nervous System, Part I, Anatomy and Physiology*. xvi + 239 pp. CIBA Pharmaceutical Company, Summit, N.J., USA.

Pilleri, G. 1959. Beitrage zur vergleichenden Morphologie des Nagetiergehirnes. *Acta Anatomica* 39 (Supplement): 1–34.

Reynolds, P.S. 2002. How big is giant? The importance of method in estimating body size of extinct mammals. *Journal of Mammalogy* 83: 321–332.

Rougier, G.W., Wible, J.R., and Hopson, J. 1992. Reconstruction of the cranial vessels in the Early Cretaceous mammal *Vincelestes neuquenianus*: implications for the evolution of the mammalian cranial vascular system. *Journal of Vertebrate Paleontology* 12: 188–216.

Rougier, G.W., Wible, J.R., and Novacek, M.J. 1996. Middle-ear ossicles of the multituberculate *Kryptobaatar* from the Mongolian Late Cretaceous: implications for mammaliamorph relationships and the evolution of the auditory apparatus. *American Museum Novitates* 3187: 1–43.

Sánchez-Villagra. 2002. The cerebeller paraflocculus and the subarcuate fossa in *Monodelphis domestica* and other marsupial mammals—ontogeny and phylogeny of a brain-skull interaction. *Acta Theriologica* 47 (1): 1–14.

Saysette, J.E. 1999. Postcranial estimators of body mass in pecoran artiodactyls. *Journal of Vertebrate Paleontology* 19 (Supplement to No. 3), Abstracts: A73.

Schaller, O. (ed.) 1992. *Illustrated Veterinary Anatomy Nomenclature*. 614 pp. Ferdinand Enke Verlag, Stuttgart.

Schmidt-Nielsen, K. 1984. *Scaling: Why is Animal Size so Important*. 241 pp. Cambridge University Press, New York.

Sereno, P. (in press). Shoulder girdle and forelimb in multituberculates: Evolution of parasagittal forelimb posture in mammals. *In*: M.T. Carrano, R.W., Blob, T.J., Gaudin, and J.R. Wible (eds.), *Amniote Paleobiology: Perspectives on the Evolution of Mammals, Birds, and Reptiles*. University of Chicago Press, Chicago.

Sereno, P. and McKenna, M.C. 1995. Cretaceous multituberculate skeleton and the early evolution of the mammalian shoulder girdle. *Nature* 377: 144–147.

Silva, M. and Downing, J.A. 1995. *CRC Handbook of Mammalian Body Masses*. 359 pp. CRC Press, Boca Raton.

Simpson, G.G. 1927. Mesozoic Mammalia, IX. The brain of Jurassic mammals. *American Journal of Science* 14: 259–268.

Simpson, G.G. 1937. Skull structure of the Multituberculata. *Bulletin of the American Museum of Natural History* 73: 727–763.

Smith, T., Guo, D.-Y., and Sun, Y. 2001. A new species of *Kryptobaatar* (Multituberculata): the first Late Cretaceous mammal from Inner Mongolia (P.R. China). *Bulletin de l'Institut royal des Sciences naturelles de Belgique, Sciences de la Terre* (Supplement 71): 29–50.

Sokal, R.R. and Rohlf, F.J. 1995. *Biometry*, 3rd edition. 887 pp. W.H. Freeman and Company, New York.

Thewissen, J.G.M. and Gingerich, P.D. 1989. Skull and endocast of *Eoryctes melanus*, a new palaeoryctid (Mammalia, Insectivora) from the early Eocene of western North America. *Journal of Vertebrate Paleontology* 9: 459–470.

Van Valkenburgh, B. 1990. Skeletal and dental predictors of body mass in carnivores. *In*: J. Damuth and B.J. MacFadden (eds.), *Body Size in Mammalian Paleobiology: Estimation and Biological Implications*, 181–205. Cambridge University Press, Cambridge, England.

Wible, J.R. and Rougier, G. 2000. The cranial anatomy of *Kryptobaatar dashzevegi* (Mammalia, Multituberculata), and its bearing on the evolution of mammalian characters. *Bulletin of the American Museum of Natural History* 247: 1–124.

Wood, B.A. 1979. An analysis of tooth and body size relationships in five primate taxa. *Folia Primatologica* 31: 187–211.

Wood, C.B. and Clemens, W.A. 2001. A new specimen and a functional reassociation of the molar dentition of *Batodon tenuis* (Placentalia, *incertae sedis*). Latest Cretaceous (Lancian), North America. *In*: F.A. Jenkins, Jr., T. Owerkowicz, and M.D. Shapiro (eds.), Studies in Organismic and Evolutionary Biology in Honor of A.W. Crompton. *Bulletin of the Museum of Comparative Zoology* 156: 99–118.

Zar, J.H. 1999. *Biostatistical Analysis*, 4 edition. 928 pp. Prentice Hall, Upper Saddle River, New Jersey.

Appendix

Rodent specimens used in body mass estimation.

Family	Species	Museum	Specimen number	Sex
Scuiridae	*Sciurus vulgaris*	UMMZ	97337	male
Scuiridae	*Sciurus carolinesis*	CM	60819	male
		CM	25230	female
Scuiridae	*Ratufa indica*	NMNH	322077	unknown
		NMNH	308415	male
Scuiridae	*Protoxerus stangeri*	NMNH	539443	female
		NMNH	539	male
Scuiridae	*Spermophilus tridecemlineatus*	CM	21155	male
		CM	61842	male
Scuiridae	*Spermophilus citellus*	UMMZ	123540	female
		NMNH	197710	unknown
Anomaluridae	*Anomalurus pusillus*	AMNH	51015	female
		AMNH	52103	male
Hystricidae	*Atherurus africanus*	UMMZ	116626	male
		NMNH	467538	female
Caviidae	*Cavia porcellus*	CM	76995	male
		UMMZ	86465	male
		UMMZ	99304	female
Dasyproctidae	*Dasyprocta leporina*	CM	40599	male
		CM	76999	unknown
		AMNH	95059	male
		AMNH	80250	male
Chinchillidae	*Chinchilla lanigera*	CM	39921	unknown
		CM	51994	unknown
		UMMZ	157198	male
		UMMZ	157197	female
Chinchillidae	*Chinchilla brevicaudata*	AMNH	17342	male
		AMNH	148467	female
Muridae	*Ondatra zibethicus*	CM	60248	male
		CM	60259	female
Muridae	*Peromyscus maniculatus*	THEW	Ht1	female
		THEW	Ht2	male

For Museum abbreviations see Institutional abbreviations (p. 178).